JPP Journal of Pharmacy and Pharmacology

Journal of Pharmacy and Pharmacology, 2021, Vol XX, 1–9
doi:10.1093/jpp/rgaa045
Research Paper
Advance Access publication 6 January 2021

OXFORD

Research Paper

Antiviral activity against Zika virus of a new formulation of curcumin in poly lactic-*co*-glycolic acid nanoparticles

María Natalia Pacho,[1] Eugenio Nahuel Pugni,[2] Johanna Briyith Díaz Sierra,[2] María Laura Morell,[2] Claudia Soledad Sepúlveda,[2] Elsa Beatriz Damonte,[2] Cybele Carina García[2,*] and Norma Beatriz D'Accorso[1]

[1]Departamento de Química Orgánica, Facultad de Ciencias Exactas y Naturales, Universidad de Buenos Aires(UBA), Centro de Investigaciones en Hidratos de Carbono (CIHIDECAR), UBA-CONICET, Buenos Aires, Argentina and [2]Laboratorio de Estrategias Antivirales, Departamento de Química Biológica, Facultad de Ciencias Exactas y Naturales, Universidad de Buenos Aires, Instituto de Química Biológica de la Facultad de Ciencias Exactas y Naturales (IQUIBICEN), UBA-CONICET, Buenos Aires, Argentina

*Correspondence: Cybele C. García, Departamento de Química Biológica, IQUIBICEN, Facultad de Ciencias Exactas y Naturales, Universidad de Buenos Aires, Ciudad Universitaria, Pabellón 2, Piso 4, 1428 Buenos Aires, Argentina. Email: cygarcia@qb.fcen.uba.ar

Received July 22, 2020; Accepted December 7, 2020.

Abstract

Objectives In the search of an effective antiviral formulation, the natural product curcumin (CUR) was encapsulated into poly(lactic-*co*-glycolic acid) nanoparticles, a non-toxic bioresorbable and biocompatible copolymer. The resulting CUR containing particles (PLGA-CUR NPs) were characterized and analysed for antiviral activity against Zika virus (ZIKV) infection.

Methods The PLGA-CUR NPs were characterized by Fourier transform infrared, differential scanning calorimetry, dynamic light scattering, scanning electron microscopy and thermogravimetric analysis and release profile. Cytotoxicity of PLGA-CUR and the antiviral activity against ZIKV were determined in Vero cells. The effect of PLGA-CUR NPs on viral RNA synthesis and protein expression was analysed by RT–qPCR and immunofluorescence staining, respectively.

Key findings The PLGA-CUR NPs showed an appropriate *in vitro* drug release profile. Our studies of the antiviral activity of PLGA-CUR NPs and CUR against ZIKV by virus yield reduction as well as viral RNA synthesis and protein expression have shown that PLGA-CUR formulation is more effective than free CUR to inhibit ZIKV infection of Vero cells.

Conclusions Our results demonstrate for the first time the antiviral activity against ZIKV of PLGA nanoparticles charged with CUR, suggesting that PLGA-CUR NPs are promising candidates for a drug formulation against human pathogenic flaviviruses.

Keywords: curcumin; antiviral activity; Zika virus; nanoparticles; poly lactic co-glycolic acid

Introduction

Zika virus (ZIKV), a member of the family *Flaviviridae* first detected in monkeys in Uganda in 1947 and later in humans, has become in recent years a relevant emerging viral infection due to its expansive spread around the world.[1] This global dissemination started from Asia to the Pacific Islands, reached Brazil in 2014 causing a major epidemic that rapidly expanded through the Americas. The main transmission route of ZIKV are the *Aedes aegypti* and *Aedes albopictus* mosquitoes, but it can be also parenterally and sexually transmitted to humans, producing outbreaks in different regions sporadically associated to neurological disorders and microcephaly.[2, 3] No vaccines or specific chemotherapy are currently available for ZIKV infection, denoting the need of effective antiviral agents.[4]

Curcumin (CUR), a hydrophobic polyphenol, is a major active component of turmeric (*Curcuma longa* L), an Indian spice of the ginger family traditionally used in Ayurvedic medicine for the treatment of various diseases. It is known that CUR has been associated with diverse medicinal properties such as antioxidant, antibacterial, antifungal, antiviral, anti-inflammatory, anticancer, pro-apoptotic and anti-atherosclerotic activities.[5, 6] These pleiotropic effects of CUR may be attributed to its ability for interaction with multiple cellular targets.[7–9] In particular, since the antiviral effectiveness of CUR was reported against several DNA and RNA viruses, including arthropod-borne viruses, this natural product is a promising candidate with very wide antiviral spectrum.[10–14]

However, the therapeutic perspectives of any agent are highly dependent on its pharmacokinetics and bioavailability at the site of action. In spite of the multiple benefits reported for CUR, several drawbacks have limited its pharmacological development for clinical use. The solubility of CUR in water under acidic and neutral conditions is very low and, additionally, high decomposition rate in alkaline media and photodegradation in water and organic solvents have been reported.[15, 16] To overcome these limitations, diverse micro- and nanocarriers have been proposed to encapsulate CUR in an improved drug delivery system.[17–22]

In this context, we have considered the use of poly lactic-*co*-glycolic acid (PLGA), a copolymer of lactic and glycolic acid, as a polymer matrix for CUR. PLGA is a very well-defined material suggested as a good drug delivery carrier because of its biodegradability, high biocompatibility, non-immunogenicity, nontoxicity, safety, improved stability of medications and possibility of sustained and/or controlled release of medicines.[23, 24] PLGA has been approved by Food and Drug Administration (FDA) and European Medicine Agency (EMA) for human use and nanomedicines. Protocols have been developed for synthesis of PLGA nanoparticles (NPs) by different methods and several drugs have been incorporated in PLGA such as folic acid, tamoxifen, neuregulin-1, carboplatin and dexamethasone.[25–28] In particular, CUR has been incorporated to PLGA generating particles that were tested in recent studies for biomedical applications, mainly in models for cancer treatment.[29–32]

In the present study, the synthesis and characterization of PLGA NPs encapsulating CUR was studied and the antiviral properties of these biological macromolecules against ZIKV infected cells were analysed. The resulting PLGA-CUR NPs were more effective than CUR to inhibit ZIKV infection, representing a novel and promising alternative formulation for the treatment of this neglected disease.

Materials and Methods

Materials

D,L-Lactide (3,6-dimethyl-1,4-dioxane-2,5-dione), glycolide, octanoic acid, dichloromethane (DCM), polyvinyl alcohol (PVA) Mw 89,000-98,000 99% hydrolysed, and CUR were purchased in Sigma-Aldrich (USA).

Synthesis of PLGA

PLGA was synthesized by opening the rings of D,L-lactide and glycolide in a bulk polymerization for 2 h at 170–175°C, under vacuum atmosphere.[33] The proportion of the stannous octoate as initiator was 0.02% and the coinitiator lauryl alcohol was 0.01% on total of monomeric mass.[34] A 50:50 D,L-lactide/glycolide ratio was used in the synthesis, considering the degradation time of these copolymers. These proportions are the most commonly used in the controlled drug delivery systems.[35]

Thermogravimetric analysis (TGA)

The test was carried out at a heating rate of 10°C/min from room temperature (±25°C) to 400°C in an unsealed platinum sample container under a nitrogen atmosphere, with a flow rate of 20°C/min. The equipment used was an SDTA 851 Mettler Toledo. The mass of the samples analysed was 3 mg.

Differential scanning calorimetry (DSC)

The DSC equipment used was a DSC Q20 TA-Instruments, COOLING RCS 90 and Tzero Pan Aluminum capsules. An unsealed aluminum sample container with nitrogen was also used as a carrier gas at a flow rate of 50 ml/min. The mass of the sample analysed was 3 mg. It was programmed to first heat the PLGA samples from room temperature (±25°C) to 150°C at a rate of 10°C/min (1st cycle) to initially eliminate the thermal history of the material. At the end of the first run, the oven was cooled with liquid nitrogen at -10°C. The equipment was then programmed for another run up to 150°C, at a heating rate of 5°C/min. The second DSC curve was the reference for determining the glass transition temperature (Tg).[36] Then, the same experimental conditions were employed for the different synthesized NPs, and results were compared with those of the PLGA bulk.

Fourier transform infrared (FTIR)

The spectra were recorded on a Nicolet IS50 FT-IR spectrometer operating in the ATR (attenuated total reflectance) mode. The infrared absorption spectra were collected at 20°C from 4000 to 450 cm^{-1}. Ten scans were performed for a resolution of 4 cm^{-1}.

Preparation of PLGA NPs and PLGA-CUR NPs

The PLGA-CUR NPs were prepared mainly by emulsion–diffusion, evaporation of the emulsion solvent, interfacial deposition and precipitation method.[37] Briefly, 40 mg of PLGA were dissolved in 5 ml of DCM with 10–15 mg of CUR by magnetic agitation. This solution was emulsified with 1% w/v PVA aqueous solution using a tip sonicator for 5 min. The resulting emulsion was mechanically stirred at 300 rpm at room temperature to enhance complete solvent evaporation. The NPs were collected by centrifugation at 200 rpm after two washes with deionized water (5 min at room temperature) to remove excess of surfactant. Thereafter, the NPs were resuspended in 1 ml of deionized water, filtered through a 40 µm filter to remove large and aggregated particles, and the filtrate was washed with cold

MilliQ water. It was frozen, and then lyophilized for 12 h. Unloaded PLGA NPs were obtained using the same technique without the addition of CUR.[27, 28]

Dynamic light scattering (DLS)

NPs were suspended and homogenized in 1 ml of distilled water to measure the hydrodynamic diameter and the polydispersity index in NanoBrook 90Plus. Then, the suspension was diluted 1:10 and loaded in a cell to request the zeta potential. The procedure was performed at room temperature (25°C).

Scanning electron microscopy (SEM)

SEM was performed to determine the size distribution and evaluate the surface morphology. The NP suspension was placed in a silicon crystal, dried in a vacuum oven and visualized with a microscope with magnification ×25 000–50 000.

Loading efficiency

Calculated amounts of PLGA-CUR NPs were dissolved in ethanol and the absorbance was recorded on UV-Vis Spectrophotometer Jenway 6700 at 425 nm.[17, 38]Uncharged PLGA NPs were used as the blank for the determination. A calibration curve, based on ethanolic 0.125–2 mg/ml CUR solutions, was used for determination of CUR loading in the PLGA-CUR NPs. Drug loading capacity and encapsulation efficiency were calculated as follows:

$$\text{Drug loading capacity (w/w \%)} = \text{(CUR /PLGA – CUR NPs) x 100}$$
$$\text{Encapsulation efficiency (\%)} = \text{(Encapsulated CUR/Initial CUR) x 100}$$

In vitro drug release

The NPs were dialysed into 3 ml of 0.1 M phosphate buffer, pH 6.5.[39] Temperature was maintained at 37°C and the release medium was gently stirred at 50 rpm. To determine the CUR release, and taking into account its low water solubility, 1 ml of the solution was extracted and replaced by 1 ml of buffer. The solution was centrifuged at 2000 rpm for 20 min to separate the released CUR that was dissolved in 3 ml of ethanol. The release experiments were performed using a Spectrophotometer Jenway 6700 with UV detection at 425 nm.[17] Samples were extracted during 120 h, at predetermined time intervals, and the determinations were done in duplicate. The released drug concentration was then calculated using the CUR standard curve as follows: Drug release (%) = (Released CUR/Total encapsulated CUR) × 100.

Cells and virus

Monkey kidney Vero cells (American Type Culture Collection, ATCC CCL-81) were propagated in Eagle's minimum essential medium (MEM) (Gibco Thermo Fisher Scientific, USA) supplemented with 5% inactivated bovine serum (Gibco). Maintenance medium (MM) consisted in MEM with 1.5% serum. C6/36 mosquito cells (ATCC CRL-1660), adapted to grow at 33°C, were cultured in L-15 medium (Leibovitz) (Gibco) supplemented with 0.3% tryptose phosphate broth, 0.02% glutamine, 1% MEM non-essential amino acids solution and 10% fetal bovine serum.

The ZIKV clinical isolate INEVH116141 (provided by the Instituto Nacional de Enfermedades Virales Humanas, Pergamino, Argentina) was propagated in C6/36 cells and titrated by plaque assay in Vero cells. For plaque assay, monolayers of confluent Vero cells were infected with 10-fold dilutions of samples containing virus at 37°C for 1 h. Following incubation, the inocula were removed, and cells were overlaid with 1 ml of MM containing 1% methylcellulose. The cells were incubated at 37°C for 3–4 days and then fixed with 4% formaldehyde. Finally, plaques were stained with 0.1% crystal violet in 20% ethanol and viral titers expressed as plaque forming units (PFU)/ml.

Cytotoxicity test

Cytotoxicity was measured by the 3-(4,5-dimethylthiazol-2-yl)-2,5-diphenyl tetrazolium bromide (MTT, Sigma-Aldrich, USA) method. Vero cells were incubated with different concentrations of CUR or PLGA-CUR NPs, respectively, for 48 h. Thereafter, cell viability was determined by addition of MTT at a final concentration 0.5 mg/ml and further incubation for 2 h. After removing cell supernatants, ethanol was added to each well to solubilize the formazan crystals and absorbance was measured in a microplate reader at 595 nm.

Antiviral assays

Antiviral activity was determined by a virus yield reduction assay. To this end, Vero cells were infected with ZIKV at a multiplicity of infection (m.o.i) of 0.1 PFU/cell and virus was adsorbed for 1 h at 37°C. Then, inocula were discarded and cells were fed with MM containing different concentrations of PLGA-CUR NPs, empty PLGA NPs, 10 µM CUR or a fixed 10 µM PLGA-CUR NPs, in the respective assays. Extracellular virus yields were determined at 48 h post-infection by a plaque assay. The effective concentration 50% (EC_{50}) was calculated as the concentration required to reduce virus yield by 50% in the PLGA-CUR NP-treated cultures compared with untreated ones. All determinations were performed in triplicate.

For qualitative cytopathic effect determination, non-infected and ZIKV-infected cell monolayers, treated or not with PLGA-CUR NPs, were inspected daily under light microscopy and after 48 h of infection, cells were fixed with 10% formaldehyde and stained with 1% crystal violet. Images were obtained using light microscopy.

Virus RNA synthesis

Vero cells were infected with ZIKV (m.o.i. 0.1 PFU/cell) and incubated with PLGA NPs, 10 µM CUR or 10 µM PLGA-CUR NPs, respectively, for 48 h. Total RNA was then extracted using TRIzol® (Invitrogen Thermo Fisher Scientific, USA) according to the manufacturer's instructions and cDNA was generated by using M-MLV (murine leukemia virus) reverse transcriptase (200 U/µl, Invitrogen Thermo Fisher Scientific, USA) and random primers. Real time PCR was employed to amplify the cDNA by using LightCycler 480 SYBR Green I Master Mix (Roche, Mannheim, Germany) detection. The NS5 viral gene was amplified using specific primers: forward 5′-CCGCTGCCCAACACAAG-3′ (1086f ZIKV) and reverse 5′-CCACTAACGTTCTTTTGCAGACAT3′ (1162 ZIKV), whereas actin was the cellular reference gene using forward 5′-GAGACCTT CAACACCCCAGCC-3′, and reverse 5′-GGCCATCTCTTGC-3′ primers. Amplification plots were expressed as Ct values and analysed with iQ5 software (BioRad, Hercules, USA).

Indirect immunofluorescence assay

Vero cells grown in coverslips were infected with ZIKV at a m.o.i. of0.1 PFU/cell and incubated with PLGA NPs, 10 µM CUR or 10 µM PLGA-CUR NPs, respectively, for 48 h. Then, cells were fixed with methanol and stained with the mouse monoclonal antibody 4G2 (Abcam, Cambridge, UK) reactive against flavivirus E protein as primary antibody, and anti-mouse immunoglobulins conjugated to isothiocyanate of fluorescein (Sigma-Aldrich, USA) as secondary

antibody. After a final washing with PBS, cells were stained with 4,6-diamidino-2-phenylindole dihydrochloride (DAPI) and visualized in an Olympus IX71 microscope. The number of cells expressing ZIKV E glycoprotein was obtained by counting positive cells in 20 fields chosen at random.

Statistical analyses

Statistical analyses were performed using GraphPad Prism software. Comparison of means was tested by one-way analysis of variance (ANOVA) with Dunnett's post test.

Statistical significance was defined as $P < 0.05$ (95% confidence interval).

Results and Discussion

Synthesis and characterization of PLGA-CUR NPs

The PLGA-CUR NPs were successfully obtained using 10 mg and 15 mg of CUR for 40 mg of PLGA, 25 % w/w (PLGA-CUR25 NPs) and 37 % w/w (PLGA-CUR37 NPs) of PLGA, respectively. The lipophilic character of CUR and the low solubility of CUR in aqueous medium are responsible for its high encapsulation efficiency, which was higher than 95% in all formulations. Then, drug loading capacity of PLGA-CUR25 and PLGA-CUR37 NPs was high, 20% w/w and 27% w/w, respectively.

The size of PLGA and PLGA-CUR NPs using SEM was 130 ± 20 and 210 ± 40 nm, respectively(Figure 1a and b), while in the experiment of DLS the determinations for CUR-PLGA NPs were 780 nm in size, a polydispersity index of 0.374 and the zeta potential was -24 ± 2 mV. The size difference between both techniques can be attributed to the aggregation of PLGA-CUR NPs in DLS since it is performed at 25°C, and as consequence a great extent of nanospheres aggregation is produced. De and Robinson[40] reported the effect of temperature on PLGA nanospheres and microspheres, and concluded that the maximal assemblage is observed when nanoparticles are small.

In the FT-IR spectrum of PLGA-CUR NPs (Figure 2a) the signals corresponding to PLGA and CUR, consistent with data reported in the literature[34] can be observed. The bands at 2946 cm^{-1} can be assigned to CH, CH_2 and CH_3 stretching in PLGA, those at 1740–1680 cm^{-1} may correspond to the C = O groups which overlaps in PLGA and CUR, those at ~1510 cm^{-1} are attributed to be aromatic stretching vibration corresponding to CUR, while the signals at ~1030 cm^{-1} are endorsed to C-OH stretching vibration.[41] These results indicate that there is no interaction between CUR and PLGA, a fact that can be explained by the chemical structure of the substances. Similar conclusion was obtained when the NPs were analysed by DSC since PLGA and PLGA-CUR NPs did not differ in the Tg (Figure 2b). Furthermore, the TGA thermograms (Figure 2c) also confirmed the lack of interaction between the polymer and CUR since there was a sum of the thermal events of both components in the charged NPs (PLGA-CUR 25 and PLGA-CUR 37).

The purpose of the encapsulation of CUR in PLGA was protecting CUR from the surrounding environment prior to its release as well as favoring this release in the desired target. On this basis, the release was evaluated favourably using phosphate buffer at pH 6.5 as the release medium, and this pH can be considered a compromise value in relation to the stability and bioavailability of CUR. Although CUR is more stable at acidic pH than at neutral or alkaline pH, its solubility decreases as pH decreases due to a change in molecular structure under acidic conditions. Then, CUR can crystallize, a phenomenon that increases with agitation because nucleation is induced, generating a predetermined measurement.[15, 16] Furthermore, the pH 6.5 is close to the pH of the intestine, which will allow oral administration with intestinal absorption of the drug. The *in vitro* drug release profile is shown in Figure 3.The initial release could be due to CUR molecules bound to the NPs surface as well as to liberation of CUR trapped in the polymeric matrix. The decrease in release at longer times suggests the importance of the diffusion process in the reaction kinetics.[17] Then, the release appears to be produced by a combination of the drug diffusion from the NPs to the external environment and the degradation of the polymer. The determination of CUR amount was optimal and 80% of CUR was released. Moreover, it should be considered that the release was carried out in an aqueous medium free of enzymes. In the human organism, the presence of enzymes able to hydrolyse PLGA to produce lactic and glycolic acid may allow a greater release of CUR in the body.

Cytotoxicity and antiviral activity of PLGA-CUR NPs

First, the cytotoxicity of both free CUR and PLGA-CUR NPs for Vero cells was comparatively evaluated after 48 h of treatment. As shown in Figure 4a, cell viability was not affected by PLGA-CUR NPs in the range of tested concentrations. Cell survival was higher than 90% in comparison to control untreated cells even up to the maximal concentration evaluated of 140 µM PLGA-CUR NPs. In contrast, a dose-dependent higher cytotoxicity was exhibited by free

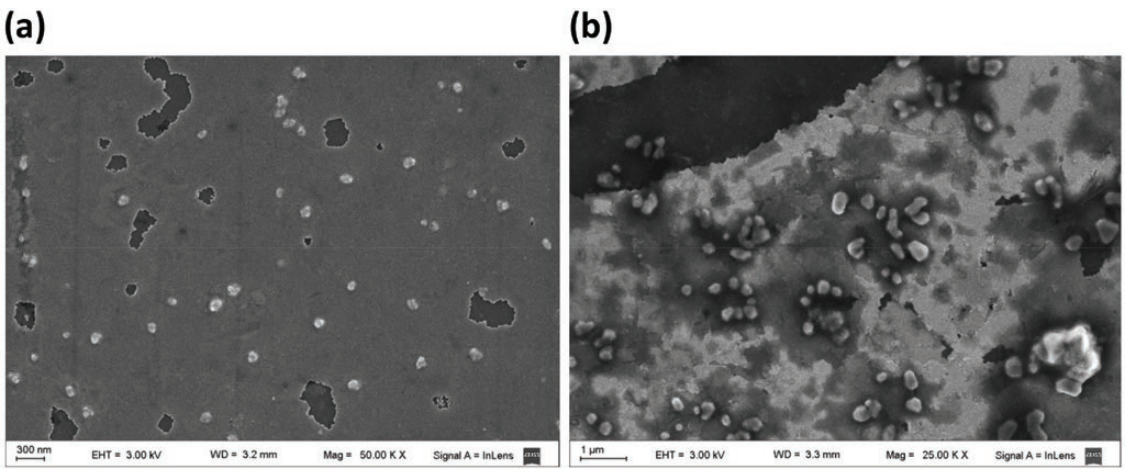

Figure 1 Scanning electron micrograph of (a) PLGA NPs and (b) PLGA-CUR NPs.

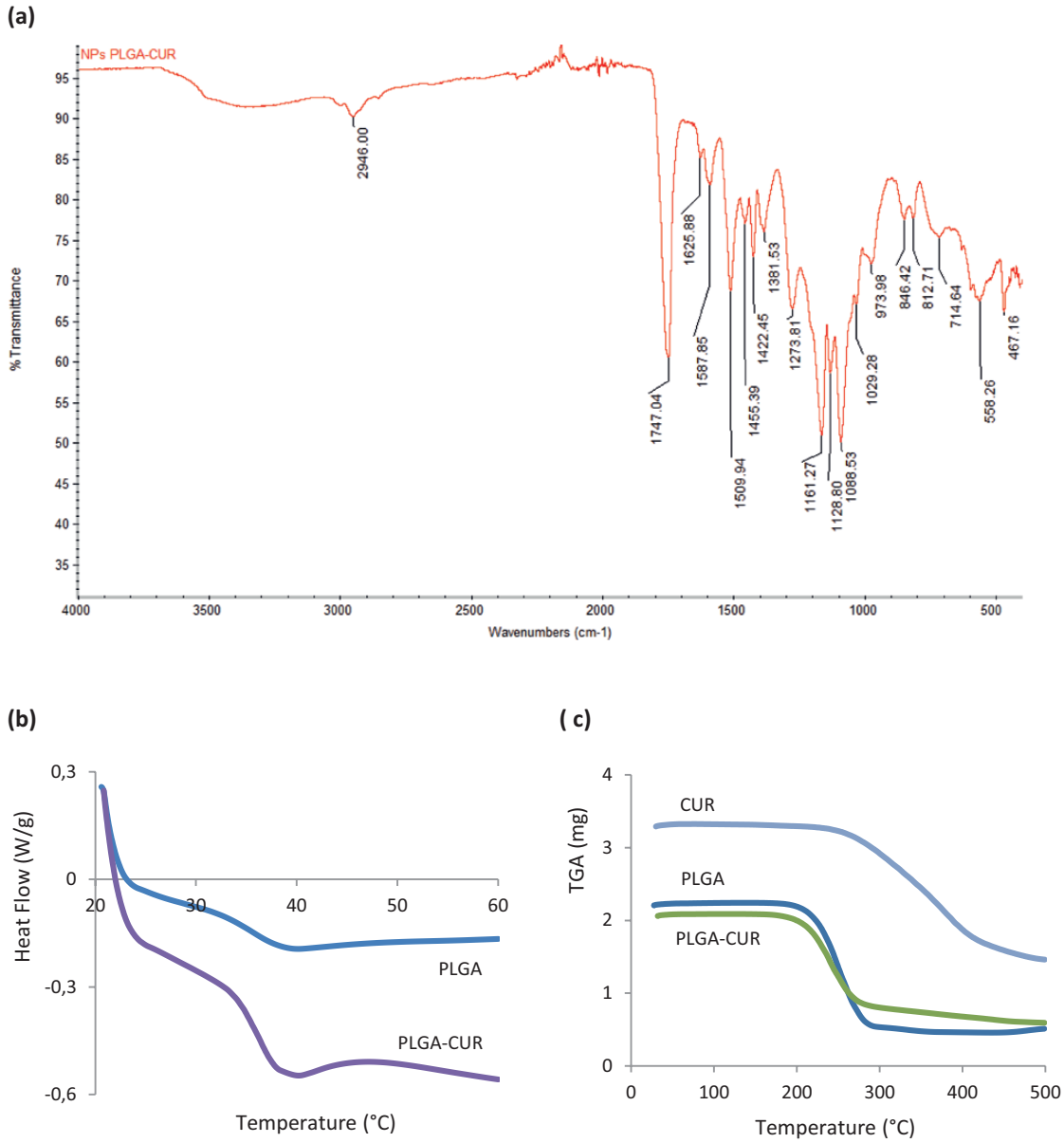

Figure 2 Characterization of nanoparticles. (a) FT-IR spectra of PLGA-CUR NPs. (b) DSC determinations of PLGA NPs and PLGA-CUR NPs. (c)TGA of CUR, PLGA NPs and PLGA-CUR NPs.

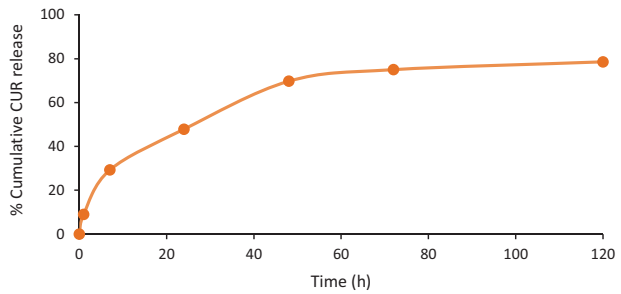

Figure 3 Release profile of CUR in ethanol at 425 nm.

CUR, attaining 50% reduction in Vero cell viability after treatment with a CUR concentration of 68.3 ± 0.4 µM.

Next, the antiviral efficacy concentration range of PLGA-CUR NPs was explored by evaluating extracellular virus production from cells infected with ZIKV (m.o.i. 0.1 PFU/cell) and treated with different concentrations of this nanoformulation. After 48 h of infection, supernatants were collected and titrated by plaque assay. In parallel, to confirm viral-induced cytopathic effect inhibition in these cultures, cell monolayers were fixed, stained and inspected in detail under light microscope.

Results from titration of supernatants denoted a dose-dependent inhibition of viral yield, showing an EC_{50} for these PLGA-CUR NPs of 3.7± 0.05 µM (Figure 4b). Given the lack of cell toxicity and the antiviral efficiency, PLGA-CUR NPs can be considered a potent and selective antiviral agent against ZIKV. In line with this, pictures from PLGA-CUR NPs treated and infected cell monolayers showed similar cell morphologies than non-infected samples, thus a complete inhibition of viral-induced cytopathic effect was found. In contrast, ZIKV infected cell monolayers showed the characteristic lytic action of ZIKV as evidenced by weak stained monolayers (Figure 4c).

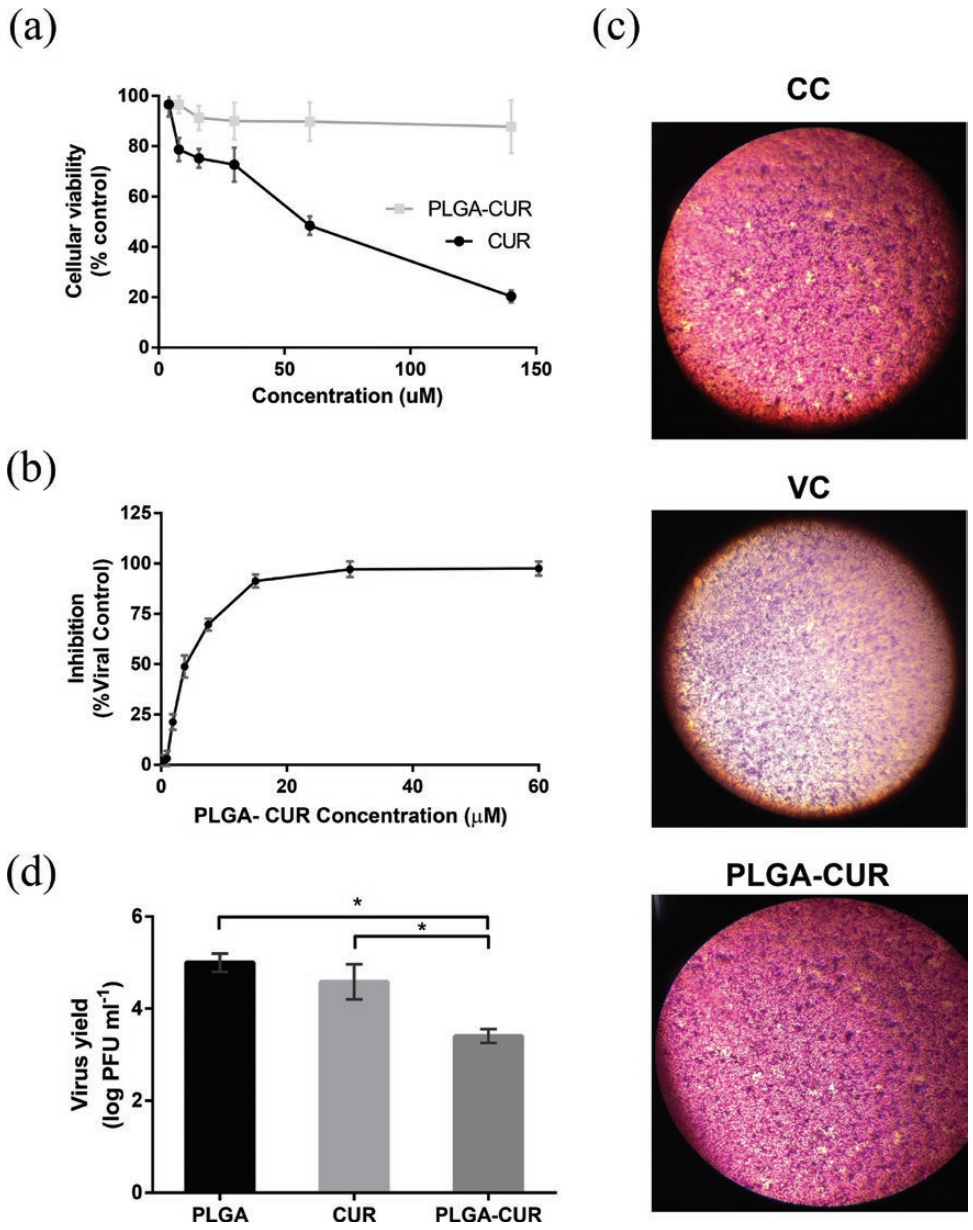

Figure 4 (a) Cytotoxicity: Vero cells were treated with different concentrations of CUR and PLGA-CUR NPs and at 48 h cellular viability was measured by MTT method. (b) Antiviral activity: Vero cells were infected with ZIKV and incubated in MM containing or not different concentrations of PLGA-CUR NPs. Virus yields were determined by plaque assay after 48 h of infection. (c) Cytopathic effect: Uninfected (cc: cell control), ZIKV infected (vc: virus control) and ZIKV infected and treated with 10 μM PLG-CUR NPs (PLGA-CUR) Vero cells were fixed with 10% formaldehyde and stained with 1% crystal violet at 48 h post-infection. (d) Comparison of PLGA-CUR and free CUR antiviral activity: Vero cells were infected with ZIKV and incubated for 48 h in the presence of PLGA NPs, 10 μM CUR or 10 μM PLGA-CUR NPs, respectively, and virus yields were determined by plaque assay. *$P < 0.05$. In (a), (b) and (d) each value is the mean of triplicate assays ± standard deviation (SD).

In order to compare the antiviral activity of these PLGA-CUR NPs with free CUR, cells were infected with ZIKV (m.o.i. 0.1 PFU/cell) and treated with empty PLGA NPs, PLGA-CUR NPs and CUR, respectively. After 48 h of infection, supernatants were collected and titrated by plaque assay. A significant inhibition of viral infection was detected in PLGA-CUR NPs treated cells in comparison to cells treated with CUR or PLGA alone (Figure 4d). The reduction in virus yield observed in ZIKV infected cells by effect of PLGA-CUR NPs in comparison to control PLGA-treated infected cells was higher than 95%. Similarly, the effectiveness of treatment with PLGA-CUR was corroborated by the increase in virus inhibition detected with respect to treatment with CUR: the compound encapsulated in NPs diminished infective ZIKV production more than 1 log with respect to free CUR (Figure 4d).

Effect of PLGA-CUR NPs on ZIKV macromolecular synthesis

The observed reduction in ZIKV titers could suggest that viral biosynthetic processes in infected cells, such as RNA replication or protein expression, could be affected by PLGA-CUR NPs. To explore this possibility, cell-associated viral genomes were quantified

by RT–qPCR at 48 h pi. As shown in Figure 5a, the synthesis of viral RNA strongly decreased in PLGA-CUR NPs treated cultures respect to non-treated ones, defined as 1. The treatment with 10 μM PLGA-CUR NPs produced a 78% reduction in viral RNA levels in ZIKV infected cells, whereas the treatment with the same concentration of free CUR only caused 29% inhibition in viral RNA, confirming the improved anti-ZIKV efficiency of encapsulated CUR.

In other set of cultures under the same experimental conditions, viral protein expression at 48 h p.i. was analysed by indirect immunofluorescence with an antibody reactive to ZIKV E glycoprotein. Here again, a very different inhibitory effect against ZIKV infection was detected between cells treated with either PLGA-CUR NPs or CUR (Figure 5b). In fact, the quantification of the number of Vero cells expressing E protein showed a 68% reduction of infected cells detected by immunofluorescence after treatment with 10 μM PLGA-CUR NPs respect to untreated ZIKV infected cultures, whereas the treatment with free CUR produced only an inhibition of 20% in the number of cells stained for E protein (Figure 5c).

In accordance with the pleiotropic targets described for CUR, the studies from different researchers have argued that the antiviral activity of this natural product may be explained by diverse mechanisms according to the virus and the host cell. The possible modes of action may imply the inhibition of a virus-related factor or the blockade of any cellular component or pathway required for virus multiplication. With respect to flaviviruses, the inhibitory effect of CUR was reported for dengue virus (DENV), another mosquito-borne flavivirus related to ZIKV, and the antiviral action was attributed to effects on cellular factors related to cytoskeleton, lipid biosynthesis and apoptosis as well as to a possible interference with enzymatic activities of DENV proteins like the polymerase NS5 and the protease complex NS2B-NS3.[14, 42, 43] A recent study described the antiviral activity of CUR against ZIKV, but the inhibition was more pronounced (about 1 log reduction in virus titer) by pretreatment of cells before infection, whereas the post-treatment with CUR affected very slightly virus infectivity.[44]

Altogether, our results in the present study demonstrated for the first time the efficiency of CUR encapsulated in PLGA nanoparticles to block ZIKV infection, with a significant improvement in antiviral activity compared with free CUR. The treatment with PLGA-CUR NPs strongly inhibited the production of infective virus particles from infected Vero cells associated with a sharp decrease in the ability of ZIKV particles to drive the biosynthesis of viral macromolecules

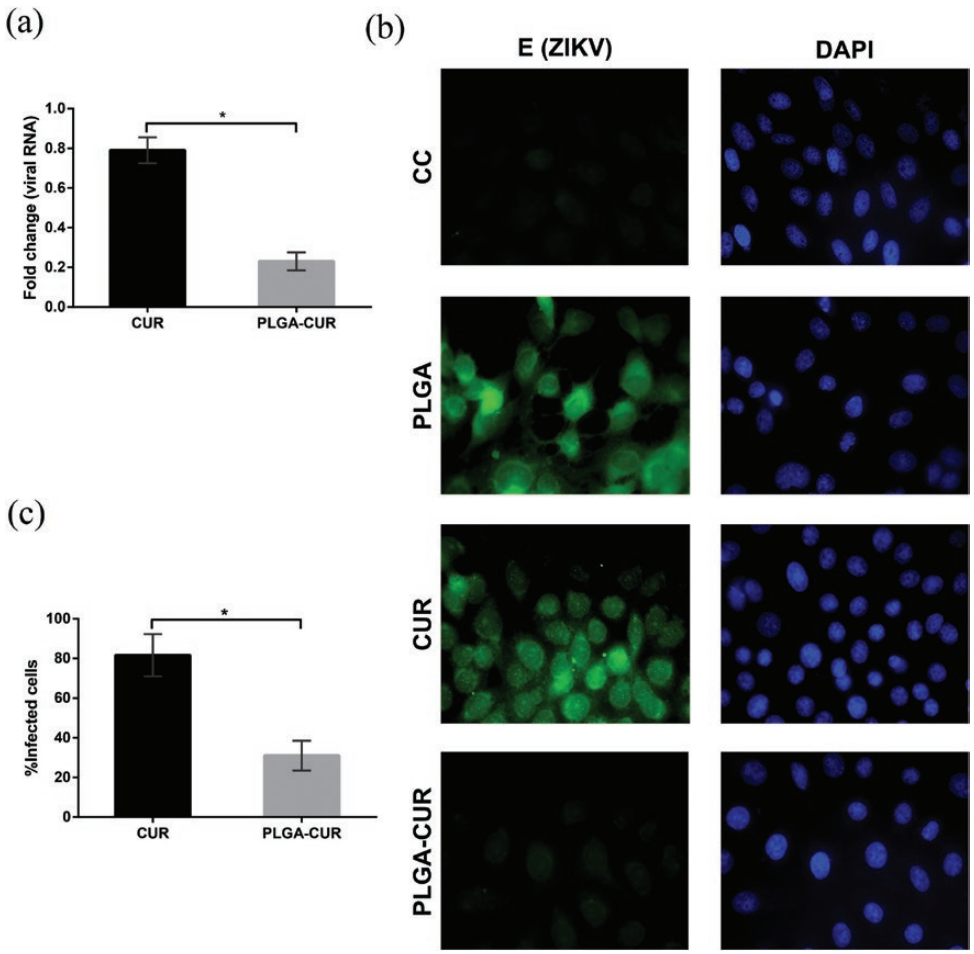

Figure 5 Effect on viral macromolecular synthesis. (a) Virus RNA synthesis: Vero cells were infected with ZIKV and treated with PLGA NPs, 10 μM CUR or 10 μM PLGA-CUR NPs. Real time RT–PCR for NS5 viral gene was performed and cellular actin gene was used for normalization. Results are expressed as fold difference viral RNA level respect to viral control for each treatment ± SD. *$P < 0.05$. (b) Virus protein expression. Vero cells were infected with ZIKV and incubated for 48 h with PLGA NPs, 10 μM of CUR or 10 μM PLGA-CUR NPs. Immunofluorescence staining was performed using anti-E ZIKV antibodies and DAPI. CC: uninfected cell control. Magnification: ×400. (c) For quantification of samples shown in (b), infected cells were counted in 20 fields chosen at random of each sample. Results are expressed as % infected cells respect to viral control ± SD. *$P < 0.05$.

within the host cell. These findings are very promising for the perspectives of the PLGA-CUR NPs for treatment of pathogenic flavivirus infection and deserve further studies in an animal model of ZIKV infection to confirm their therapeutic potential.

Conclusions

CUR was adequately encapsulated in PLGA nanoparticles. There was no interaction between CUR and the copolymer in the resulting PLGA-CUR NPs that showed a satisfactory release profile. Thus, both properties support the methodology for its application.

The evaluation of the inhibitory activity of PLGA-CUR NPs and CUR here performed by virus yield reduction assay, viral RNA synthesis and protein expression has shown that PLGA-CUR formulations were significantly more effective than free CUR to inhibit ZIKV infection of Vero cells. Our results demonstrate for the first time the selected antiviral activity against ZIKV of PLGA nanoparticles charged with CUR, suggesting that PLGA-CUR NPs are promising candidates for a drug formulation against human pathogenic flaviviruses.

Acknowledgments

We thank all members of the laboratories involved for helpful advice and discussions.

Funding

This work was supported by Universidad de Buenos Aires (UBA) (20020130100021BA and 20020170100363BA), Consejo Nacional de Investigaciones Científicas y Tecnológicas (CONICET) (PIP112-2015-0100443CO, 298/14 and PIP11220170100171CO) and Agencia Nacional de Promoción Científica y Tecnológica, Argentina (PICT 2015 3080). CSS, CCG, EBD and NBD are members of the Research Career from CONICET; MNP and JBDS are fellows from CONICET; MLM was supported by doctoral fellowship from UBA.

References

1. Gubler DJ *et al*. History and emergence of Zika virus. *J Infect Dis* 2017; 216: S860–7.
2. Mlakar J *et al*. Zika virus associated with microcephaly. *N Engl J Med* 2016; 374: 951–8.
3. doRosário MS *et al*. Guillain-Barré syndrome after Zika virus infection in Brazil. *Am J Trop Med Hyg* 2016; 95: 1157–60.
4. Masmejan S *et al*. Zika virus, vaccines, and antiviral strategies. *Expert Rev Anti-infect Ther* 2018; 16: 471–83.
5. Zhou H *et al*. The targets of curcumin. *Curr Drug Targets* 2011; 12: 332–47.
6. Hewlings SJ, Kalman DS. Curcumin: a review of its' effects on human health. *Foods* 2017; 6: 92.
7. Dairaku I *et al*. Inhibitory effect of curcumin on IMP dehydrogenase, the target for anticancer and antiviral chemotherapy agents. *Biosci Biotechnol Biochem* 2010; 74: 185–7.
8. Shakeri A *et al*. Curcumin: a naturally occurring autophagy modulator. *J Cell Physiol* 2019; 234: 5643–54.
9. Hasima N, Aggarwal BB. Cancer-linked targets modulated by curcumin. *Int J Biochem Mol Biol* 2012; 3: 328–51.
10. Kutluay SN *et al*. Curcumin inhibits herpes simplex virus immediate-early gene expression by a mechanism independent of p300/CBP histone acetyltransferase activity. *Virology* 2008; 373: 239–47.
11. Chen TY *et al*. Inhibition of enveloped viruses infectivity by curcumin. *PLoS One* 2013, 8: 62482.
12. Kim K *et al*. Curcumin inhibits hepatitis C virus replication via suppressing the Akt-SREBP-1 pathway. *FEBS Lett* 2010; 584: 707–12.
13. Ali A, Banerjea AC. Curcumin inhibits HIV-1 by promoting Tat protein degradation. *Sci Rep* 2016; 6: 27539.
14. Balasubramanian A *et al*. Inhibition of dengue virus by curcuminoids. *Antiviral Res* 2019; 162: 71–8.
15. Kumavat SD *et al*. Degradation studies of curcumin. *Int J Pharm Sci Rev Res* 2013; 3: 50–5.
16. Kharat M *et al*. Physical and chemical stability of curcumin in aqueous solutions and emulsions: impact of pH, temperature, and molecular environment. *J Agric Food Chem* 2017; 65: 1525–32.
17. Rejinold NS *et al*. Curcumin-loaded biocompatible thermoresponsive polymeric nanoparticles for cancer drug delivery. *J Colloid Interface Sci* 2011; 360: 39–51.
18. Li X *et al*. Preparation and in-vitro/in-vivo evaluation of curcumin nanosuspension with solubility enhancement. *J Pharm Pharmacol* 2016; 68: 980–8.
19. Alizadeh N, Malakzadeh S. Antioxidant, antibacterial and anti-cancer activities of β- and γ-CDs/curcumin loaded in chitosan nanoparticles. *Int J Biol Macromol* 2020; 147: 778–91.
20. Lachowicz D *et al*. Blood-compatible, stable micelles of sodium alginate-curcumin bioconjugate for anti-cancer applications. *Eur Polym J* 2019; 113: 208–19.
21. Medel S *et al*. Curcumin-bortezomib loaded polymeric nanoparticles for synergistic cancer therapy. *Eur Polym J* 2017; 93: 116–31.
22. Gutiérrez-Gutiérrez F *et al*. Encapsulation of curcumin into layered double hydroxides improve their anticancer and antiparasitic activity. *J Pharm Pharmacol* 2020; 72: 897–908.
23. Molavi F *et al*. Polyester based polymeric nano and microparticles for pharmaceuticalpurposes: a review on formulation approaches. *J Control Release* 2020; 320: 265–82.
24. Park K *et al*. Injectable, long-acting PLGA formulations: analyzing PLGA and understanding microparticle formation *J Control Release* 2019; 304: 125–34.
25. Santhosh KT *et al*. Design and optimization of PLGA microparticles for controlled and local delivery of Neuregulin-1 in traumatic spinal cord injury. *J Control Release* 2017; 261: 147–62
26. Zhong H *et al*. A comprehensive map of FDA-approved pharmaceutical products. *Pharmaceutics* 2018; 10: 263.
27. Kumari A *et al*. Biodegradable polymeric nanoparticles based drug delivery systems. *Colloid Surface B* 2010; 75: 1–18.
28. Chevalier MT *et al*. Non-covalently coated biopolymeric nanoparticles for improved tamoxifen delivery. *EurPolym J* 2017; 95: 348–57.
29. Dwivedi P *et al*. Core–shell microencapsulation of curcumin in PLGA microparticles: programmed for application in ovarian cancer therapy. *Artif Cells Nanomed Biotechnol* 2018; 46: S481–91.
30. Ayyanaar S *et al*. A novel curcumin-loaded PLGA micromagnetic composite system for controlled and pH-responsive drug delivery. *Colloids Surf A Physicochem Eng Asp* 2019; 573: 188–95.
31. Zaman MS *et al*. Curcumin nanoformulation for cervical cancer treatment. *Sci Rep* 2016; 6: 20051.
32. Gracia E *et al*. Impregnation of curcumin into a biodegradable (poly-lactic-co-glycolic acid, PLGA) support, to transfer its well known in vitro effect to an in vivo prostate cancer model. *Nutrients* 2019; 11: 2312.
33. D'Avila C *et al*. Synthesis and characterization of poly(D,L-lactide-co-glycolide) copolymer. *J Biomater Nanobiotechnol* 2012; 3: 208–25.
34. Bendix D. Chemical synthesis of polylactide and its copolymers for medical applications. *Polym Degrad Stabil* 1998; 59: 129–35.
35. Chasin M, Langer R. *Biodegradable polymers as drug delivery systems*, 1st edn, New York: McGraw-Hill, 1990.
36. Scarpa MV *et al*. Thermal behavior and stability of biodegradable spray-dried microparticles containing triamcinolone. *Int J Pharm* 2009, 368: 45–55.
37. Arranz-Romera A *et al*. Simultaneous co-delivery of neuroprotective drugs from multi-loaded PLGA microspheres for the treatment of glaucoma. *J Control Release* 2019; 297: 26–38.

38. Petrov PD *et al*. Multifunctional block copolymer nanocarriers for co-delivery of silver nanoparticles and curcumin: synthesis and enhanced efficacy against tumor cells. *Eur Polym J* 2016; 81: 24–33.
39. Colthup NB *et al*. *Introduction to infrared and raman spectroscopy*, 2nd edn, New York: Academic Press, 1975.
40. De S, Robinson DH. Particle size and temperature effect on the physical stability of PLGA nanospheres and microspheres containing Bodipy. *AAPS Pharm Sci Tech* 2004; 5: 18–24.
41. Okagu OD *et al*. Utilization of insect proteins to formulate nutraceutical delivery systems: encapsulation and release of curcumin using mealworm protein-chitosan nano-complexes. *Int J Biol Macromol* 2020; 151: 333–43.
42. García Ariza LL *et al*. Molecular cloning, modelling and docking with curcumin of the dengue virus 2 NS5 polymerase domain. In: Castillo L, Cristancho M, Isaza G, Pinzón A, Rodríguez J (eds), *Advances in Computational Biology.* Cham: Springer, 2014; 273–8.
43. Padilla SL *et al*. Inhibitory effects of curcumin on dengue virus type 2-infected cells in vitro. *Arch Virol* 2014; 159: 573–9.
44. Mounce BC *et al*. Curcumin inhibits Zika and chikungunya virus infection by inhibiting cell binding. *Antiviral Res* 2017; 142: 148–57.